Physics

Electricity & Magnetism fields

Okayama University

Year 1984

Influence of lamination orientation and stacking on magnetic characteristics of grain-oriented silicon steel laminations

Takayoshi Nakata
Okayama University

N. Takahashi
Okayama University

Y. Kawase
Okayama University

N. Nakano
Okayama University

INFLUENCE OF LAMINATION ORIENTATION AND STACKING ON MAGNETIC CHARACTERISTICS

OF GRAIN-ORIENTED SILICON STEEL LAMINATIONS

T. Nakata, N. Takahashi, Y. Kawase and M. Nakano

ABSTRACT

Analytical and experimental investigations have been carried out upon the behaviour of flux in laminations, where the rolling directions of adjacent sheets are reversed. The paper clarifies the mechanism of the greatly different magnetic characteristics between such laminations and usual ones, where the rolling directions of adjacent sheets are coincident.

1. INTRODUCTION

At the T-joint of a so-called scrap-less-type three-phase transformer core, laminations are alternatively turned over so that the angle between the rolling directions of overlapping sheets may become 90°. The magnetic characteristics of such laminations are greatly different from those of usual laminations, where the rolling directions of adjacent sheets are coincident [1], [2]. Some measurements of flux have been carried out in order to obtain a fuller understanding of the effect of the stacking method of laminations [3]-[5]. If localized flux distributions are obtained, the mechanism of the different magnetic characteristics in these laminations should be explained clearly.

The flux distribution in laminations, where the rolling directions are reversed, is calculated using a new approximation method to solve three-dimensional magnetic fields [6]. Using a single sheet tester [7], the experimental investigations have also been carried out on the effects of stacking, cut angle and the flux density. The paper clarifies the mechanism of the greatly different magnetic characteristics.

2. ANALYSIS

2.1 Model

For simplicity, laminations stacked as shown in Fig. 1 were examined. These laminations were tested in the single sheet tester. The stackings in Figs. 1 (a) and 1 (b) are called as the "//" and "X" stackings respectively. For example, "X" stacking in Fig. 1(b) corresponds to the hatched parts of a so-called scrap-less-type three-phase transformer core shown in Fig. 2. The solid arrows ⟵⟶ denote the rolling directions of the sheets in the first lamination and the dashed arrows ⟵----⟶ denote those in the adjacent lamination.

The laminations in Fig. 1 were 0.3(mm) thick highly-oriented silicon steel M-3H (AISI-78). The frequency was 50(Hz).
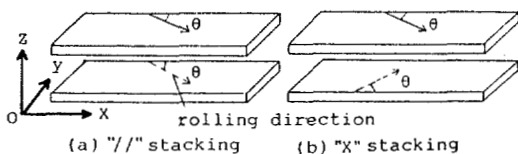

(a) "//" stacking   (b) "X" stacking

Fig. 1 Stacking methods.

The authors are with the Department of Electrical Engineering, Okayama University, Okayama 700, Japan.
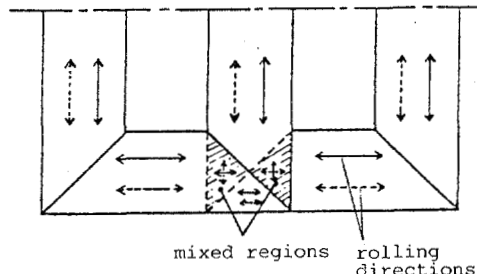
mixed regions   rolling directions

Fig. 2 Three-phase transformer core.

2.2 Method of Analysis

The magnetic characteristics of the "//" stacking shown in Fig. 1(a) were analyzed using the two-dimensional finite element method [8].

As the flux distribution in the lamination shown in Fig. 1(b) is nonuniform in the z-direction, three-dimensional analysis is required. If it is possible to analyze this three-dimensional field approximately by modifying the two-dimensional finite element method, both the computer storage and the computing time can be reduced considerably. The "new approximation method [6]" developed by the authors is used in the analysis of the "X" stacking.

In this approximation method, the flux distribution in each lamination is calculated from vector potentials {A} as well as distribution ratios F_{X_1} and F_{y_1} defined later [6]. It is assumed that the z-directional magnetic resistance is negligibly small.

X-and y-directional components of flux densities, i.e. B_{X_1}, B_{y_1}, B_{X_2} and B_{y_2}, in the first and the second sheets in Fig. 3 are denoted by

$$B_{X_1} = \Phi_X F_{X_1}/t \qquad (1)$$

$$B_{X_2} = \Phi_X (1 - F_{X_1})/t \qquad (2)$$

$$B_{y_1} = \Phi_y F_{y_1}/t \qquad (3)$$

$$B_{y_2} = \Phi_y (1 - F_{y_1})/t \qquad (4)$$

where, Φ_X and Φ_y are x- and y-directional components of the total flux of the two sheets. "t" is the effective thickness of one sheet in the z-direction. F_{X_1} and F_{y_1} are the ratios of the x- and y-directional components of the flux in the first sheet to Φ_X and Φ_y respectively. The flux distribution in each lamination is calculated from the following equations:

$$\frac{\partial X}{\partial A_i} = 0 \quad , \quad \frac{\partial X}{\partial F_{X_1}} = \frac{\partial X}{\partial F_{y_1}} = 0 \qquad (5)$$

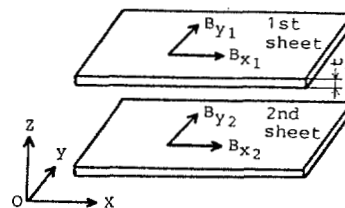Where, A_i is the vector potential at a node i. X is given by

Fig. 3 Flux density in each sheet.

$$X = X_1 + X_2 \tag{6}$$

$$X_1 = t \iint_S (\int_0^{B_{X_1}} \nu_{X_1} B_{X_1} dB_{X_1} + \int_0^{B_{y_1}} \nu_{y_1} B_{y_1} dB_{y_1}) dxdy \tag{7}$$

$$X_2 = t \iint_S (\int_0^{B_{X_2}} \nu_{X_2} B_{X_2} dB_{X_2} + \int_0^{B_{y_2}} \nu_{y_2} B_{y_2} dB_{y_2}) dxdy \tag{8}$$

X_1 and X_2 are the energies in the first and the second sheets.

2.3 Method of Experiment

Figure 4 shows the single sheet tester used in the experiment [7]. As this tester has two yokes, the magnetic characteristics of the laminations stacked with two sheets having different cut angles can be investigated. The iron loss was measured using B and H coils [9]. The H coils are set at the upper and lower sides of the two sheets as shown in Fig. 4. The length of the H coil is 2/3 of that of the exciting coil. The B coil is set between the exciting coil and the H coil, and its length is exactly the same as that of the H coil. The interlaminar gap length T_g was adjusted by inserting a sheet made of phenol resin.
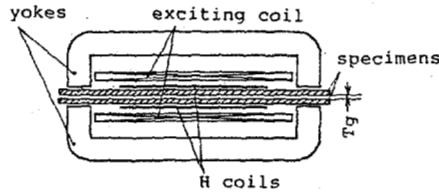

Fig. 4 Single sheet tester.

3. RESULTS AND DISCUSSIONS

Figure 5 shows the effects of the stacking, the cut angle θ shown in Fig. 1, and the maximum flux density B_m, on the iron loss W. These curves were obtained by using the single sheet tester shown in Fig. 4. The iron loss is greatly affected by the stacking method. The mechanism of the different iron loss characteristics is clarified by the localized flux distributions shown in Figs. 6 and 7 which are calculated for the case of $\theta = 45°$.

In Fig. 6, one flux line represents 0.1(Wb) when the width and the thickness of the sheet are equal to 1.0(m) respectively. The flux in the "//" stacking flows in a direction deviating from the rolling one.
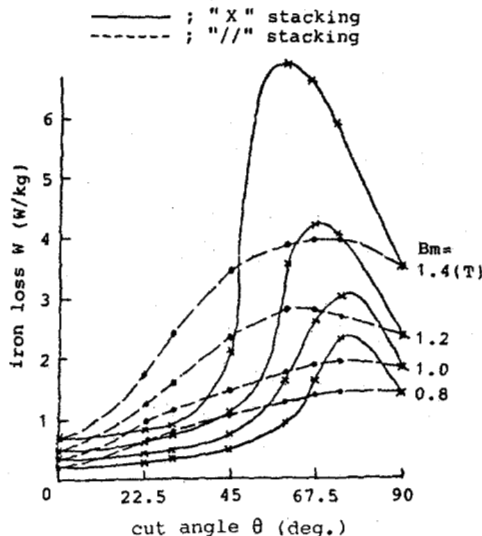

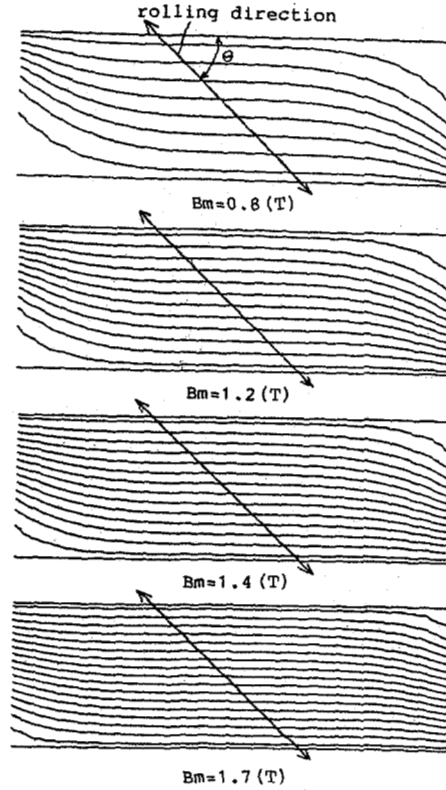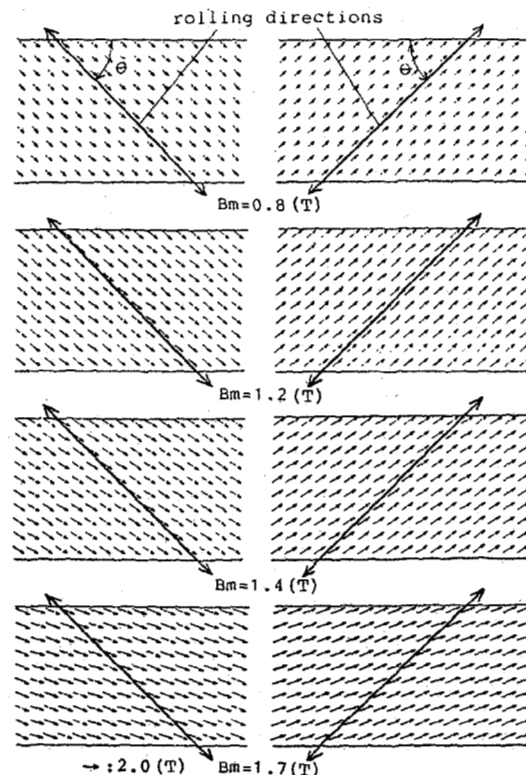Fig. 5 Angle dependence of iron loss ($T_g \approx 0$(mm), measured).

Fig. 6 Flux distributions of "//" stacking ($\theta = 45°$).

(a) the first sheet   (b) the second sheet

Fig. 7 Flux distributions of "X" stacking ($\theta = 45°$).

In the "X" stacking, the flux zigzags transversing to the adjacent sheet as shown in Fig. 7. The flux does not flow continuously in the sheet. It transverses to the adjacent sheet, and changes the direction about 2θ, so that the flux in each sheet may flow in the rolling direction. When the gap length Tg becomes smaller, most of the transversing flux concentrates near the edge of the sheet. From the above-mentioned reason, the flux distribution should be represented by flux density vectors as shown in Fig. 7 instead of the flux lines in Fig. 6.

Figure 8 shows the relationship among the apparent flux density vector Bm and the flux density vectors B_1 and B_2 in the first and the second sheets of the "X" stacking. The apparent flux density Bm is the mean vector of the flux densities B_1 and B_2. The amplitudes B_1 and B_2 of them are denoted by

$$B_1 = B_2 = Bm / \cos \varphi \qquad (9)$$

where, φ is the angle between vectors B_1 (or B_2) and Bm as shown in Fig. 8. When Bm is small, the angle φ is nearly the same as θ. According to Eq. (9), B_1 or B_2 is nearly equal to $\sqrt{2}Bm$ in the case of Fig. 7. When Bm is increased, φ becomes smaller than θ. Because the magnetic resistance in the φ direction is smaller than that in the θ directio˙ due to the magnetic saturation in this θ direction. . Fig. 7, the flux deviates from the rolling direction ˙hen Bm$\geq$1.2(T). Although, Eq. (9) means that B_1 or B_2 reaches infinity when θ approaches 90°, B_1 or B_2 cannot be increased so much because of the magnetic saturation. From this reason, B_1 (or B2) approaches a saturated value, and finally reaches Bm when θ=90°. The iron loss characteristics in Fig. 5 can be explained from the above-mentioned facts.

Figure 9 shows the estimated iron loss [10] in the case of Fig. 7. When Bm<1.2(T), the estimated iron loss curve denoted by the solid line agrees well with the measured one denoted by the dashed line. When Bm$\geq$1.2(T), the iron loss estimated is not reliable. Because the flux does not flow in the rolling direction and an accurate estimation method of the iron loss for such a case is not established yet.

The flux distribution in Fig. 7 is checked indirectly by examining the iron loss characteristics of the laminations with the interlaminar gap Tg shown in Fig. 4. When the gap Tg is increased, the iron loss of the "X" stacking approaches that of the "//" stacking as shown in Fig. 10. Because the transverse flux in the interlaminar gap decreases with the increase of Tg.
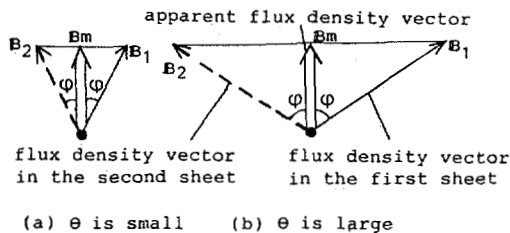

Fig. 8 Flux density vectors.

(a) θ is small   (b) θ is large

flux density vector in the second sheet

flux density vector in the first sheet
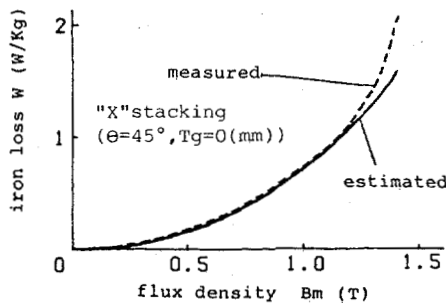
apparent flux density vector

Fig. 9 Measured and estimated iron losses.

Figures 9 and 10 prove indirectly that the calculated flux distributions shown in Figs. 6 and 7 are sufficiently reasonable. The iron loss characteristics in Fig. 5 are explained by such an extraordinary behaviour of the fluxes clarified from Figs. 6 and 7.
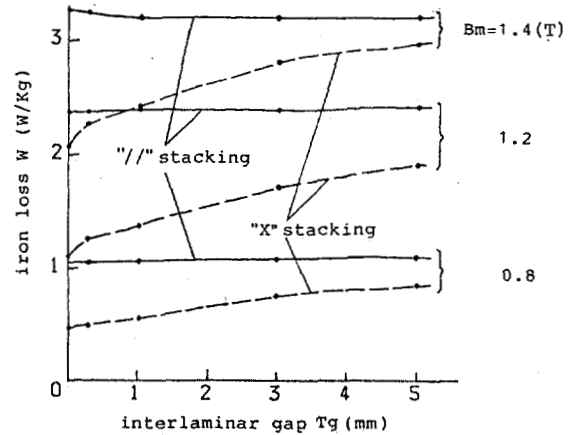

Fig. 10 Effects of the interlaminar gap Tg
(measured, θ=45°).

4. CONCLUSIONS

The uniqueness of magnetic characteristics of laminations, where the rolling directions in adjacent sheets are reversed, is explained by investigating the behaviour of flux in such laminations analytically and experimentally. The knowledge of the detailed behaviour of the flux obtained in this paper should give useful suggestions to reduce the iron loss in the T-joints of transformer cores.

The behaviour of flux in laminations with various cut angle will be reported later.

REFERENCES

[1] J. Slama, "Investigation of Magnetic Interactions between Oriented SiFe Sheets", Journal of Magnetism and Magnetic Materials, 41, 1-3 (1984).

[2] Nippon Steel Corporation, "Technical Report ORIENTCORE·HI-B", 148 (1973).

[3] A.J. Moses and P.S. Phillips, "Effects of Stacking Methods on Epstein-Square Power-Loss Measurements", Proc. IEE, 124, 4, 413 (1977).

[4] D. Davies and A.J. Moses, "Causes of Some Errors in Measurements in Grain-Oriented Silicon-Iron Using the Epstein Square", Journal of Magnetism and Magnetic Materials, 26, 1-3, 35 (1982).

[5] A.J. Moses, "Factors Affecting Localised Flux and Iron Loss Distribution in Laminated Cores", Journal of Magnetism and Magnetic Materials, 41, 1-3 (1984).

[6] T. Nakata, Y. Kawase and M. Kawata, "Approximate Solution of Three-Dimensional Magnetic Field at Joints of Transformer Cores", Papers of Combined Technical Meeting on Rotating Machines and Static Apparatus, RM-83-92, SA-83-43, IEE, Japan (1983).

[7] T. Nakata, Y. Ishihara, N. Takahashi and Y. Kawase, "Analysis of Magnetic Field in a Single Sheet Tester Using an H Coil", Journal of Magnetism and Magnetic Materials, 26, 1-3, 179 (1982).

[8] T. Nakata and N. Takahashi, "The Finite Element Method in Electrical Engineering", Tokyo, Morikita Publishing Co. Ltd. (1982) (book).

[9] W. Brix, K.A. Hempel and W. Schroeder, "Method for the Measurement of Rotational Power Loss and Related Properties in Electrical Steel Sheets", IEEE Trans. on Magnetics, MAG-18, 6, 1469 (1982).

[10] T.Nakata and N.Takahashi,"Finite Element Analysis of Transformer Cores", Memoirs of the School of Engineering, Okayama University, 18 (1984).